



LAWRENCE
LIVERMORE
NATIONAL
LABORATORY

Atmospheric Stability Affects Wind Turbine Power Collection

S. Wharton, J. K. Lundquist

April 26, 2011

Environmental Research Letters

Disclaimer

This document was prepared as an account of work sponsored by an agency of the United States government. Neither the United States government nor Lawrence Livermore National Security, LLC, nor any of their employees makes any warranty, expressed or implied, or assumes any legal liability or responsibility for the accuracy, completeness, or usefulness of any information, apparatus, product, or process disclosed, or represents that its use would not infringe privately owned rights. Reference herein to any specific commercial product, process, or service by trade name, trademark, manufacturer, or otherwise does not necessarily constitute or imply its endorsement, recommendation, or favoring by the United States government or Lawrence Livermore National Security, LLC. The views and opinions of authors expressed herein do not necessarily state or reflect those of the United States government or Lawrence Livermore National Security, LLC, and shall not be used for advertising or product endorsement purposes.

1 **Atmospheric Stability Affects Wind Turbine Power Collection**

2

3 Sonia Wharton¹ and Julie K. Lundquist^{2,3}

4

5 ¹Atmospheric, Earth and Energy Division, Lawrence Livermore National Lab, P.O. Box 808, L-103,
6 Livermore, CA 94551,

7 ²Department of Atmospheric and Ocean Sciences, University of Colorado at Boulder, CUB-311, Boulder,
8 CO 80309,

9 ³National Renewable Energy Laboratory, Golden, CO, 80401

10

11

12

13

14

15

16 **LLNL-JRNL-481323**

17 **Short title:** Atmospheric stability influences wind power

18 **Keywords:** wind turbines, wind power, atmospheric stability, wind shear, turbulence

19

20 **Abstract**

21

22 Power generated by a wind turbine largely depends on wind speed. During time periods with
23 identical hub-height wind speeds but different shapes to the wind profile, a turbine will produce different
24 amounts of power. This variability may be induced by atmospheric stability, which affects profiles of
25 mean wind speed, direction, and turbulence across the rotor disk. Our paper examines turbine power
26 generation data, segregated by atmospheric stability, to investigate power performance dependencies at a
27 West Coast North American wind farm. The dependency of power on stability is clear, regardless of
28 whether time periods are segregated by 3-dimensional turbulence, turbulence intensity, or wind shear.
29 Power generated at a given wind speed is higher during stable conditions and lower during strongly
30 convective conditions: average power output differences approach 15%. Wind energy resource
31 assessment and day ahead power forecasting could benefit from increased accuracy if atmospheric
32 stability impacts are measured and appropriately incorporated in power forecasts, i.e., through generation
33 of power curves based on a range of turbulence regimes.

34

35 **PACS:** 92.60.Fm, 92.60.Gn, 88.50.G-, 88.50.J-

36 1. Introduction

37 While the average wind speed in a turbine rotor disk largely determines the amount of power that
38 is generated, wind shear and turbulence intensity also influence power output (e.g., Motta *et al.* 2005,
39 Sumner and Masson 2006, Gottschall and Peinke 2008, van den Berg 2008). A dependency of power
40 performance on atmospheric stability has been observed previously (Christensen and Dragt 1986,
41 Fransden 1987, Elliott and Cadogan 1990, and Rohatgi and Barbezier 1999), although few of these
42 studies have analyzed power output from modern turbines with hub heights above 60 m. More recently,
43 studies have focused on the sensitivity of power curves to stability-related characteristics including wind
44 shear (Raeshide *et al.* 2009, Wagner *et al.* 2009,) and turbulence intensity (Kaiser *et al.* 2003, Honhoff
45 2007, Tindal *et al.* 2008).

46 Conclusions vary dramatically on the effects of stability on power generation. At a U.S. Great
47 Plains wind farm, Raeshide *et al.* (2009) found that moderate to high positive wind shear led to higher
48 power output than when wind shear was low. In contrast, a modeling study by Wagner *et al.* (2009),
49 based on turbines on flat Danish terrain, suggested that very high positive wind shear decreased power by
50 26%, as compared to no shear conditions. As stability also is related to atmospheric turbulence, others
51 have suggested that separate power curves for different turbulent conditions be calculated to distinguish
52 the effects of turbulence on power production (Elliott and Cadogan 1990). This may be especially
53 important for downwind turbines within wind farms, as chaotic and turbulent wake flows increase stress
54 on downstream turbines (Mann *et al.* 2008). Despite such studies, power curves are usually presented as a
55 function of hub-height wind speed alone, without information on wind velocity and turbulence intensity
56 across the rotor disk (IEC 2003).

57 In our study, we quantify the influence of atmospheric stability on power performance using wind
58 profile data from a 3-axis Sonic Detection and Ranging (SODAR), investigating a full range of stability
59 parameters including turbulence kinetic energy (*TKE*), vertical turbulence intensity (I_v), horizontal
60 turbulence intensity (I_h), and the wind shear coefficient (α). The stability parameters are described in

61 detail in Wharton and Lundquist (in press). This present study is the first paper to our knowledge to
62 explore the relationship between 3-dimensional turbulence and turbine power production.

63

64 **2. Data and Methods**

65 *2.1 Wind farm overview*

66 Power data from July 2007 to June 2008 were collected at a multi-MW wind farm in western
67 North America at an elevation near sea-level. Strong land-ocean temperature differences, particularly
68 during the summer, drive strong local southwesterly winds. The landscape is grass-covered rolling hills,
69 with subtle elevation changes. In addition to turbine power data, meteorological data from an 80 m tall
70 tower, SODAR, and turbine-mounted cup anemometers were also used. A map of the wind farm and
71 instrument locations is found in Wharton and Lundquist (in press).

72 A subset of 80 m tall, horizontal-axis, three-bladed wind turbines, with rotor diameters of
73 approximately 80 m, was selected for analysis. The turbines are pitch controlled. The exact type and
74 make of turbines is not disclosed here for proprietary reasons. The turbines were selected to ensure that
75 they did not experience wakes from other turbines or upwind hills, i.e., the distance between an upwind
76 obstacle and downwind turbine was verified to ensure that the turbine was no closer than four rotor
77 diameters (IEC 2003). The turbines generated power based on the wind between 40 m and 120 m above
78 ground level (AGL). Hub-height (80 m) wind speed was measured with cup anemometers (NRG IceFree,
79 NRG Systems, Hinesburg, VT, USA) located downwind of each turbine's nacelle hub.

80 The meteorological tower was equipped with cup anemometers at 50, 60, and 80 m AGL to
81 measure wind speed at a sampling rate of 1 Hz and accuracy of 0.3 m s^{-1} . High resolution vertical profiles
82 of wind speed, direction, and 3-dimensional turbulence were available from a three beam, 4500 Hz
83 Doppler mini SODAR (Model4000, Atmospheric Systems Corporation, Santa Clarita, CA, USA). The
84 SODAR measured 3-axis wind speeds (u , v , and w), with a sampling rate of 1 Hz per beam and a vertical
85 resolution of 10 m, from 20 m to 200 m AGL. The data were quality-controlled according to accepted
86 SODAR standards (e.g. Antoniou *et al.* 2003) (see Wharton and Lundquist in press).

87 2.2 Assessment of atmospheric stability

88 A dimensionless wind shear exponent (α) was calculated from wind speed at two heights 1 and 2
89 using the simple power law (Elliott *et al.* 1987):

90
$$U_2(z) = U_1 \left(\frac{z_2}{z_1} \right)^\alpha \quad (1)$$

91 where U is mean horizontal wind speed (m s^{-1}) at height z (m). The wind shear exponent approximates
92 atmospheric stability but it is not a direct measure of stability. Separate wind shear exponents were
93 calculated across heights of 50 and 80 m at the meteorological tower and from the SODAR at heights of
94 40 and 80 m (bottom half of a turbine rotor disk), 80 and 120 m (top half), and 40 and 120 m (entire disk).

95 Turbulence intensity (I_U , %) includes direct measurements of horizontal turbulence fluctuations in
96 the wind field. Turbulence intensity was calculated from a cup anemometer:

97
$$I_{U_cup} = \frac{\sigma_U}{U} \quad (2)$$

98 where U is mean horizontal wind speed (m s^{-1}) at 80 m and σ_U is standard deviation (m s^{-1}) of U at 80 m
99 over a ten-minute averaging period. SODAR estimates of turbulence intensity also were calculated:

100
$$I_{U_SODAR} = \frac{\sqrt{(\sigma_u^2 + \sigma_v^2)}}{U} \quad (3)$$

101 where σ_u^2 is variance in latitudinal wind speed (u , m s^{-1}) and σ_v^2 is variance in longitudinal wind speed (v ,
102 m s^{-1}). In both equations, higher I_U magnitudes indicate more turbulence in the wind field. Note that
103 I_{U_cup} and I_{U_SODAR} are different quantities, as discussed in Wharton and Lundquist (in press).

104 Some investigators have reported tendencies for SODARs to overestimate horizontal velocity
105 variances (e.g., Gaynor and Kristensen 1986, Ito 1997) which would lead to higher turbulence estimates;
106 however, these errors are not included in the vertical velocity component. Therefore, a SODAR vertical
107 turbulence intensity (I_w , %) was calculated based on standard deviations in the vertical velocity (σ_w) at 80
108 m:

109
$$I_w = \frac{\sigma_w}{U} \tag{4}$$

110 Lastly, related to turbulence intensity, turbulence kinetic energy (*TKE*, $\text{m}^2 \text{s}^{-2}$) was calculated from the
 111 SODAR:

112
$$TKE = \frac{1}{2}(\sigma_u^2 + \sigma_v^2 + \sigma_w^2) \tag{5}$$

113 where σ_u^2 , σ_v^2 , and σ_w^2 are variance in latitudinal (*u*), longitudinal (*v*), and vertical (*w*) velocities (m s^{-1}) at
 114 80 m. *TKE* is a direct measure of the intensity of 3-dimensional turbulence.

115 In prior work, we documented confidence in the SODAR stability parameters via a comparison
 116 with a robust measurement of stability, the Obukhov length (*L*) and classified each ten-minute period as
 117 belonging to one of five stability classes: strongly stable, stable, near-neutral (includes slightly stable,
 118 neutral, and slightly convective), convective, or strongly convective (see Wharton and Lundquist in
 119 press). Thresholds for each stability class and descriptions of related boundary layer conditions are listed
 120 in table 1.

121
 122 *2.3 Evaluation of power performance*

123 Power curves (turbine power output versus wind speed) were calculated using ten-minute
 124 averages of power (kW) from each of the six turbines. Manufacturer’s (“expected”) power curves
 125 provided comparisons to the wind farm observations. The amount of power theoretically available to a
 126 turbine, at time *i*, is expressed as the energy flux (*P_i*, Watts):

127
$$P_i = 0.5\rho_a A_i U_i^3 \tag{6}$$

128 where ρ_a is air density (kg m^{-3}), A_i is area of a turbine rotor disk (m^2), and U_i is instantaneous wind speed
 129 (m s^{-1}). However, the extraction of power from the wind is not 100% efficient and the theoretical,
 130 maximum mechanical efficiency of a turbine is just 59.3% (Betz 1966).

131 In our study, power performance by an individual turbine was evaluated using normalized power
 132 (P_{norm} , %):

133
$$P_{norm}(t,i) = \frac{P_{t,i}}{P_{rated}} \times 100 \quad (7)$$

134 where $P_{t,i}$ is the average amount of power (kW) generated at turbine t over a 10 minute time period i and
 135 P_{rated} is the maximum amount of power (kW) that turbine t is potentially able to produce, as determined
 136 by the manufacturer. A P_{norm} of 100% indicates that a turbine produced power equal to the
 137 manufacturer's maximum rating. P_{norm} was calculated for each of the six turbines for every 10
 138 minute period.

139

140 *2.4 Calculation of equivalent wind speed*

141 Hub-height wind speed may not represent the flow across the entire rotor disk. Recent work by
 142 Wagner *et al.* (2009) and Antoniou *et al.* (2007) suggest calculating a speed representative of the disk
 143 area for use in power curves. Following Sumner and Masson (2006), 10-minute average SODAR data, at
 144 nine measurement heights from 40-120 m, were used to calculate a rotor-averaged or equivalent wind
 145 speed (U_{equiv_SODAR} , m s⁻¹) across heights representing the rotor disk:

146
$$U_{equiv_SODAR} = \frac{2}{A_t} \int_{H-r}^{H+r} U(z)(r^2 - H^2 + 2Hz - z^2)^{1/2} dz \quad (8)$$

147 where $U(z)$ is mean wind speed (m s⁻¹) at height z (m), r is radius of the rotor disk (m), H is hub-height
 148 (m), z is measurement height (m), and dz is 10 m. This integral over the rotor disk altitudes was evaluated
 149 via summation using the SODAR data at discrete 10 m vertical intervals. Only vertical variability is
 150 measured and included in this interval as horizontal homogeneity is assumed.

151 Further, following Wagner *et al.* (2009), Eq (8) was modified to recognize that the instantaneous
 152 wind speed is a composite of both mean (U) and turbulent (σ_U) components. To incorporate any turbulent
 153 energy encountered by the rotor, a modified "true-flux" equivalent wind speed ($U_{equivTI_SODAR}$, m s⁻¹) was
 154 calculated:

155
$$U_{equivTI_SODAR} = \frac{2}{A_t} \int_{H-r}^{H+r} U_I(z) (r^2 - H^2 + 2Hz - z^2)^{1/2} dz \quad (9)$$

156 where wind speed at each height $U_I(z)$ has now been “corrected” to include any additional energy from
 157 turbulence:

158
$$U_I(z) = \sqrt[3]{U^3(z)(1 + 3I_U^2)} \quad (10)$$

159 Note that Eq (9) assumes that the wind turbine is able to extract energy from turbulent motions in
 160 the air stream.

161 The SODAR was located between 3 and 4.8 km from the turbines discussed, making it difficult to
 162 justify directly using the SODAR “true-flux” equivalent wind speed in the power curves. To adjust for
 163 any localized differences in wind speed between SODAR and turbines, we first assumed that differences
 164 between SODAR hub-height wind speed U_{80_SODAR} and SODAR “true-flux” equivalent wind speed
 165 $U_{equivTI_SODAR}$ could be considered a constant (over a 10 minute period) across the wind farm. Next, the
 166 turbine nacelle (80 m) wind speed $U_{nacelle}$ at each turbine was “corrected” for the presence of wind shear
 167 and turbulence as observed by the SODAR. This correction led to a nacelle “true-flux” equivalent wind
 168 speed ($U_{equivTI_nacelle}$, $m\ s^{-1}$):

169
$$U_{equivTI_nacelle} = U_{nacelle} + (U_{equivTI_SODAR} - U_{80_SODAR}) \quad (11)$$

170 $U_{equivTI_nacelle}$ was calculated for each 10 minute period and for each individual turbine.

171

172 **3. Results**

173 *3.1 Climatology and stability*

174 Significant seasonal and diurnal variations in wind speed and power production were present at
 175 this wind farm, i.e., wind speeds were higher at night (more power) than during the day (less power) and
 176 higher during the warm season (more power) than in the cool season (less power). For all six turbines,
 177 average nighttime P_{norm} was 23% in winter, 46% in spring, 67% in summer, and 27% in autumn. Average
 178 daytime P_{norm} was 20% in winter, 35% in spring, 43% in summer, and 20% in autumn (figure 1).

179 This site exhibited stable, near-neutral, and convective stability conditions in a 37:17:44 ratio
180 during the spring and summer. As expected, SODAR stability parameters indicated that daytime hours
181 were almost always strongly convective, convective or near-neutral, while nights were strongly stable,
182 stable, or near-neutral. During very stable conditions, wind shear was significant, positive, and averaged
183 3.5 m s^{-1} between the bottom and top of the rotor disk. During convective conditions, wind shear was
184 negligible and suggested a well mixed surface layer.

185

186 *3.2 Estimate of rotor disk wind speed*

187 We compared four measurements of wind speed: (1) nacelle cup anemometer 80 m U , (2)
188 SODAR 80 m U , (3) SODAR “true-flux” equivalent U , and (4) nacelle-adjusted “true-flux” equivalent U .
189 Figure 2 shows the frequency distribution of spring and summer wind speeds for each U . The frequency
190 distribution shifted toward lower wind speeds in the nacelle-based measurements as compared to
191 SODAR. This shift likely is due to turbine wake effects on the nacelle cup anemometer (the anemometer
192 is behind the turbine blades) and is most prevalent in the 6 to 9 m s^{-1} range when all turbulence classes
193 are included (figure 2a) but erodes during high turbulence periods (figure 2c). Differences between hub-
194 height wind speed and the “true-flux” rotor-averaged wind speed did not account entirely for the
195 frequency shift between the two instruments. This behavior suggests that the differences in wind speed
196 were instrument-driven or location-driven. Small wind speed differences between hub-height wind speed
197 and “true-flux” equivalent wind speed are evident in both the nacelle and SODAR data. While these
198 differences are small, they are important for wind power in the region where power generation is related
199 to the wind speed cubed (~ 4 to 12 m s^{-1}). Differences were most acute for wind speeds below 3 m s^{-1}
200 (irrelevant for wind power) and for wind speeds between 8 and 11 m s^{-1} .

201 To discern the appropriate U for power curves, 10-minute power data P_{norm} are plotted as a
202 function of (a) nacelle cup anemometer 80 m U , (b) nacelle cup anemometer “true-flux” equivalent U , (c)
203 SODAR 80 m U , and (d) SODAR “true-flux” equivalent U for a typical summer day in figure 3. The
204 uncertainty induced by a non co-located SODAR wind speed in the power curves can be seen in figures

205 3c and 3d. When compared with the manufacturer's power curve, the SODAR-based power curves have
206 lower Pearson's coefficient (r) values ($r = 0.88-0.89$) than the nacelle-based ($r = 0.94-0.95$). Furthermore,
207 a small improvement (in terms of a higher r value and lower standard deviation of residuals) is evident
208 from using the nacelle-adjusted "true-flux" equivalent wind speed instead of the nacelle hub-height U
209 (figure 3b). Though small, these differences suggest that the nacelle-adjusted "true-flux" equivalent wind
210 speed generates the most accurate power curves at this site.

211

212 *3.3 Stability-stratified power curves*

213 To examine stability-related effects on turbine power performance, 10-minute power generation
214 data were segregated into stability classes, based on the wind shear exponent (section 3.3.1), turbulence
215 intensity (3.3.2), or turbulence kinetic energy (3.3.3) per the categories defined in table 1. Normalized
216 power P_{norm} is plotted as a function of binned nacelle "true-flux" equivalent wind speed with separate
217 curves for each stability class. Data points are missing in the power curves when there were too few 10-
218 minute data to statistically represent the 0.5 m s^{-1} wind speed bin. Error bars indicate one standard
219 deviation in power for each velocity bin and stability classification. The power curves shown in all
220 figures are for one turbine, Turbine 1, but are representative of all six turbines examined. Also, the power
221 curves include only strongly stable/stable, convective, or strongly convective regimes to highlight the
222 most distinct power generation differences. Because the warm season is the primary wind power season at
223 this site, the power curves include spring and summer months only.

224

225 *3.3.1 Wind shear*

226 Using four wind shear parameters (α_{120_40} , α_{120_80} , α_{80_40} , and α_{80_50}), 10-minute P_{norm} data from
227 Turbine 1 were stratified according to stability regime (figure 4). Wind shear in the top half of the rotor
228 disk (α_{120_80}) did not significantly impact power production – the power curves for the three stability
229 classes are nearly indistinguishable (figure 4c). However, differences in power production emerge when
230 P_{norm} was stratified by cup anemometer α_{80_50} (figure 4a) or SODAR α_{80_40} (figure 4b) at heights in the

231 lower half of the rotor disk, or from using wind shear representing the entire disk (α_{120_40}) (figure 4d). For
232 example, average P_{norm} during wind speeds of 8 m s^{-1} was $39\% \pm 5\%$ during strongly convective
233 conditions and $48\% \pm 4\%$ during stable or strongly stable conditions as compared to an expected P_{norm} of
234 41% (figure 4d). High amounts of wind shear (i.e., stable/strongly conditions) in the lower half or entire
235 rotor disk led to 9% more power produced on average by the turbine as compared to periods of negative
236 shear (i.e., strongly convective conditions) for wind speeds between 6 to 10 m s^{-1} .

237

238 3.3.2 Turbulence intensity

239 The utility of SODAR measurements for understanding power performance is more apparent
240 when considering turbulent intensity. Power curves for Turbine 1 were stratified by nacelle cup
241 anemometer I_U and SODAR I_U in figure 5. Stratification by nacelle I_U (figure 5a) included stable or
242 strongly stable periods ($I_U < 10\%$) and convective or strongly convective periods ($I_U > 13\%$). Too few
243 data points were available to isolate the effects of strongly convective conditions for the nacelle-based
244 parameter. Observed power yields followed the expected power curve regardless of stability class. Power
245 differences were less than 5% and occurred when the nacelle “true-flux” equivalent wind speed was
246 between 4 and 7 m s^{-1} .

247 In contrast, distinct power curves emerged when the power data were stratified by SODAR-
248 measured I_U (figure 5b). Figure 5b shows power generation data segregated into stable or strongly stable
249 ($I_U < 10\%$), convective ($13\% I_U < 20\%$), or strongly convective ($I_U > 20\%$) conditions. The most
250 significant power curve differences occurred between very stable /stable and very convective conditions
251 for wind speeds 7.0 to 8.5 m s^{-1} . In general, Turbine 1 over-performed during stable/strongly stable
252 conditions for 5.5 to 8 m s^{-1} wind speeds and under-performed during strongly convective conditions for
253 all wind speeds above 5.5 m s^{-1} . Greatest under-performance occurred at moderate wind speeds (7.0 to
254 8.5 m s^{-1}) during strongly convective conditions. For example, for a wind speed of 7.5 m s^{-1} , mean P_{norm}
255 was $40\% \pm 6\%$ during strongly stable/stable conditions and $23\% \pm 4\%$ during strongly convective
256 conditions, compared to the expected P_{norm} of 33% . Among all six turbines examined, differences in

257 normalized power between stable/strongly stable (more power) and strongly convective (less power)
258 conditions ranged from 10-20%.

259 Extraneous noise (e.g., spikes in the measurements) may occur in the SODAR horizontal velocity
260 data and could exaggerate power distinctions. To remove this possible bias in the I_U power curves, power
261 data were stratified by vertical turbulence intensity I_w . Power data were binned into stable or strongly
262 stable conditions ($I_w < 6\%$), convective conditions ($9\% < I_w < 17\%$), or strongly convective conditions (I_w
263 $> 17\%$) (figure 6). Power deficiencies were observed for every wind speed above turbine cut-in speed (U
264 $> 3.5 \text{ m s}^{-1}$) during strongly convective conditions. Under-performance was particularly high for winds
265 between $10.5\text{-}11 \text{ m s}^{-1}$; Turbine 1 produced just 75% of expected power. Over-performance was less
266 evident during stable/strongly stable conditions and reached + 3% in the $5 \text{ to } 8 \text{ m s}^{-1}$ wind speed range.

267

268 3.3.3 Turbulence kinetic energy

269 Distinct power differences also emerged when P_{norm} was stratified by TKE . The most significant
270 power deviations occurred during strongly convective conditions ($TKE > 1.4 \text{ m}^2 \text{ s}^{-2}$); these differences
271 approached 18% between expected power and the amount of power produced (figure 7). For example, at
272 9 m s^{-1} , average P_{norm} was $44\% \pm 10\%$ during strongly convective conditions, as compared to an expected
273 P_{norm} of 60%. During stable/strongly stable conditions ($TKE < 0.7 \text{ m}^2 \text{ s}^{-2}$), over-performance was smaller
274 than observed with either SODAR-based I_U (figure 5b) or α (figure 4d) and approached + 5%.

275

276 4. Discussion

277 Data from a well-instrumented wind farm enabled assessment of atmospheric stability impacts on
278 power generation. This study builds on stability-related, rotor disk wind speed trends presented in
279 Wharton and Lundquist (in press) for a megawatt wind farm. Other wind power studies have determined
280 atmospheric stability based on one or two stability parameters, e.g., Motta *et al.* (2005) and van den Berg
281 (2008), while ours is the first study to our knowledge that relates power production to a large set of
282 independent stability parameters, including SODAR-derived I_w and TKE . Previous studies into the

283 influence of stability on wind power have not found universal agreement (e.g., Hunter *et al.* 2001,
284 Antoniou *et al.* 2009). In our study, we found that high wind shear ($\alpha > 0.2$) had a positive effect on
285 power production for the 5 to 10 m s⁻¹ range, while negative wind shear had a negative impact on power
286 except for wind speeds above 12 m s⁻¹. For low-to-moderate wind speeds (< 5 m s⁻¹), we observed that
287 wind shear had little impact on power performance. For the 5-8.5 m s⁻¹ wind range, we found that very
288 high amounts of turbulence decreased power production by an average of 15%. This result contradicts
289 observations made by Elliott and Cadogan (1990) who found that higher turbulence led to more power for
290 wind speeds between 4 and 8 m s⁻¹. However, their site experienced different stability-related
291 meteorological conditions than the one examined here. In their study, the rotor-averaged wind speed was
292 less than hub-height wind speed under stable conditions. Therefore, less energy was available to turbines
293 during stable conditions than during convective. In contrast, we found a higher rotor-averaged wind
294 speed than hub-height wind speed under stable conditions and, consequently, greater energy production.
295 We observed a negative impact of turbulence on power production: power decreased as the boundary
296 layer became more convective, coinciding with a lower “true-flux” equivalent wind speed, higher
297 turbulence, and small or negative wind shear across the rotor disk. It is important to note that our location
298 experiences strong, channeled flow in the spring and summer months. Therefore, our stable conditions did
299 not experience the strong veering of the wind vector with height (i.e., directional shear) as is common at
300 locations with nocturnal low-level jets (e.g., Banta *et al.* 2002). Strong directional shear can undermine
301 the performance of a turbine, which might explain why some studies find under-performance during
302 stable conditions at high wind speeds (Rareshide *et al.* 2009). At our location, however, we consistently
303 and repeatedly observed under-performance during strongly convective conditions.

304 It is important to consider that atmospheric turbulence and wind shear are intrinsically related,
305 e.g., turbulence erodes to shear and shear leads to turbulence. As such, the exact effects of turbulence on
306 power generation versus wind shear on generation are hard to distinguish. A low turbulence intensity
307 parameter generally includes conditions with high wind shear and vice versa, while a low wind shear
308 parameter usually occurs during times of high turbulence. To distinguish the individual effects of

309 turbulence versus wind shear on power production, very high time resolution (> 10 Hz) turbulence
310 measurements are needed so that the coherent structures of turbulence can be properly identified.
311 Unfortunately, such data were not available to us at this wind farm but this topic warrants further
312 investigation for other sites.

313

314 Based on our findings, we offer these recommendations:

315 *4.1 Accurate power curves require a “true-flux” equivalent wind speed*

316 Due to variability in wind shear and turbulence, a significant source of error or uncertainty in
317 power curves will be generated by differences between the true disk-averaged velocity and hub-
318 height velocity. These errors may appear in modeling studies as well, and simulations, such as
319 Wang and Prinn (2010) reported, must account for variations of atmospheric stability when
320 considering power performance of turbines.

321

322 *4.2 Nacelle-based measurements do not lend insight into power differences*

323 Nacelle-based turbulence intensity did not enable useful distinctions of stability regimes
324 to isolate influences on power production. This finding is supported by the weak
325 correlation between nacelle I_U and the Obukhov length stability parameter
326 (Wharton and Lundquist in press) and studies by Hölling et al. (2007), Finnigan (2002),
327 and Kline (2008) which show that cup anemometers are unable to measure high
328 turbulence even in controlled wind tunnels. Instruments with higher accuracy and
329 sampling frequency are needed in wind power studies.

330

331 **5. Conclusions**

332 This work highlights the benefit of observing nearly complete profiles of wind speed and
333 turbulence across the turbine rotor disk. Here, the presence of a nighttime, stable boundary layer, with
334 little or no directional shear, had the same effect on power performance as increasing the wind velocity at

335 hub-height by 0.2 m s^{-1} . The opposite was true for strongly convective conditions. Very high turbulence
336 and low shear had the same effect on power as decreasing hub-height wind speed by $0.5\text{-}1.0 \text{ m s}^{-1}$. These
337 results suggest that wind energy resource assessment and short-term (day ahead) power forecasting would
338 likely benefit from increased accuracy if atmospheric stability impacts are measured and appropriately
339 incorporated in power forecasts, such as through generation of power curves based on a range of
340 turbulence regimes.

6. Acknowledgements

The authors express appreciation to Iberdrola Renewables, Inc. for sharing their wind farm data. We also acknowledge helpful suggestions by Neil Kelley and Dennis Elliott of NREL. This work was funded by the Department of Energy's Wind and Water Power Program Office under the Renewable Systems Interconnect Support Program (BNR-EB2502010) and performed under the auspices of the U.S. Department of Energy by Lawrence Livermore National Laboratory under Contract DE-AC52-07NA27344. LLNL is operated by Lawrence Livermore National Security, LLC, for the DOE, National Nuclear Security Administration under Contract DE-AC52-07NA27344. NREL is a national laboratory of the U.S. Department of Energy, Office of Energy Efficiency and Renewable Energy, operated by the Alliance for Sustainable Energy, LLC.

7. References

- Antoniou I, Jørgensen H E, Ormel F, Bradley S, von Hünenbein S, Emeis S and Warmbier G 2003 *On the theory of SODAR measurement techniques* (Risø National Laboratory: Roskilde, Denmark) p 59
- Antoniou I, Wagner R, Pedersen S M, Paulsen U, Madsen H A, Jørgensen H E, Thomsen K, Enevoldsen P and Thesbjerg L 2007 Influence of wind characteristics on turbine performance. *In: Scientific proceedings* (European Wind Energy Conference and Exhibition Milan: Italy)
- Antoniou I, Pedersen S M and Enevoldsen P D 2009 Wind shear and uncertainties in power curve measurement and wind resources *Wind Engineer.* **33** 449-468
- Banta R M, Newsom R K, Lundquist J K, Pichugina Y L, Coulter R L and Mahrt L 2002 Nocturnal low-level jet characteristics over Kansas during CASES-99 *Bound.-layer Meteor.* **105** 221-252.
- Betz A 1966 *Introduction to the theory of flow mechanics* (Oxford, England: Pergamon Press) p 281
- Christensen C J and Dragt J B (ed) 1986 *Accuracy of power-curve measurements*. Risø-M-2632 (Risø National Laboratory, Roskilde: Denmark)
- Elliott D L, Holliday C, Barchet W, Foote H and Sandusky W 1987 *Wind energy resource atlas of the United States* (DOE/CH 10093-4, Golden, Colorado: Solar Energy Research Institute) p 210
- Elliott D L and Cadogan J B 1990 Effects of wind shear and turbulence on wind turbine power curves *In: Scientific proceedings* (European Community Wind Energy Conference and Exhibition Madrid: Spain)
- Finnigan J J 2002 Instrumentation II: Vector Wind Sensors, *In: Advanced short course on agricultural, forest and micro meteorology* (ed) Rossi F, Duce P, Spano D (Sassari, Italy: Consiglio Nazionale Delle Ricerche) pp 160-171
- Fransden S 1987 On uncertainties in power performance measurements *In: Scientific Proceedings 6th ASME Wind Energy Symposium*, American Society of Mechanical Engineers, New York

- Gaynor J E and Kristensen L 1986 Errors in second moments estimated from monostatic Doppler Sodar winds, Part II: Application to Field Measurements *J Atmos Ocean. Technol.* **3** 529-534
- Gottschall J and Peinke J 2008 How to improve the estimation of power curves for wind turbines *Environ. Res. Lett.* **3** 1-7
- Hölling M, Schulte B, Barth S and Peinke J 2007 Sphere anemometer – a faster alternative solution to cup anemometry, The Science of Making Torque from Wind *J Phys Conference Series* **75** 012064.
- Honhoff S 2007 Power Curves – The effect of environmental conditions *In: Scientific proceedings (GE Wind AWEA Wind Speed and Energy Workshop, Portland, Oregon USA)*
- Hunter R, Pedersen T F, Dunbabin P, Antoniou A, Frandsen S, Klug H, Albers A and Lee W K 2001 *European wind turbines testing procedure developments. Task 1: Measurement method to verify wind turbine performance characteristics* (Risø National Laboratory, Roskilde, RISOE R-1209)
- International Electromechanical Commission (IEC) 2003 *Wind turbine generator systems part 12-1: power performance measurements of grid connected wind turbines* Draft Technical Report No IEC 61400-12-1
- Ito Y 1997 Errors in wind measurements estimated by five-beam array Doppler Sodar *J Atmos Ocean. Technol.* **14** 792-801
- Kaiser K, Hohlen H and Langreder W 2003 Turbulence correction for power curves *In: Scientific proceedings (European Wind Energy Conference and Exhibition, Madrid: Spain)*
- Kline J 2008 Addressing bias in wind measurements: Part 1 *In: Scientific proceedings (AWEA Wind Resource and Project Energy Assessment Workshop, Portland, Oregon USA)*
- Mann J, Sorensen J N and Morthorst P-E 2008 Editorial: Wind energy *Environ. Res. Lett.* **3** 015001
- Motta M, Barthelmie R J and Vølund P 2005 The influence of non-logarithmic wind speed profiles on potential power output at Danish offshore sites *Wind Energy* **8** 219-236

- Rareshide E, Tindal A, Johnson C, Graves A M, Simpson E, Blegg J, Harris T and Schoborg D 2009 Effects of complex wind regimes on turbine performance *In: Scientific proceedings (American Wind Energy Association WINDPOWER Conference, Chicago, Ill USA)*
- Rohatgi J and Barbezier G 1999 Wind turbulence and atmospheric stability – their effects on wind turbine output *Renewable Energy* **16** 908-911
- Sumner J and Masson C 2006 Influence of atmospheric stability on wind turbine power performance curves *J. Sol. Energy Eng.* **128** 531-537
- Tindal A, Johnson C, LeBlanc M, Harman, K, Rareshide, E and Graves A-M 2008 Site-specific adjustments to wind turbine power curves. *In: Scientific proceedings (American Wind Energy Association WINDPOWER Conference, Houston, Texas USA)*
- van den Berg G P 2008 Wind turbine power and sound in relation to atmospheric stability *Wind Energy* **11** 151-169
- Wagner R, Antoniou I, Pedersen S M, Courtney M S and Jørgensen H E 2009 The influence of the wind speed profile on wind turbine performance measurements *Wind Energy* **12** 348-362
- Wang C and Prinn R G 2011 Potential climatic impacts and reliability of large-scale offshore wind farms *Environ. Res. Lett.* **6** 025101
- Wharton S and Lundquist J K Assessing atmospheric stability and its impacts on rotor-disk wind characteristics at an onshore wind farm *Wind Energy* DOI: 10.1002/we.483, in press

Tables

Stability class	Boundary layer properties	Hub-height wind speed	Wind shear	Turbulence
strongly stable	Highest shear in swept-area, nocturnal LLJ may be present, little turbulence except just below the LLJ	strong, especially at night	highest: $\alpha > 0.3$	lowest: $I_U < 8\%$; $I_w < 4\%$; $TKE < 0.4 \text{ m}^2 \text{ s}^{-2}$
stable	High wind shear in swept-area, low amount of turbulence unless a nocturnal LLJ is present	strong, especially at night	high: $0.2 < \alpha < 0.3$	low: $8\% < I_U < 10\%$; $4\% < I_w < 6\%$; $0.4 < TKE < 0.7 \text{ m}^2 \text{ s}^{-2}$
near-neutral	Logarithmic wind profile	generally strongest	moderate: $0.1 < \alpha < 0.2$	moderate : $10\% < I_U < 13\%$; $6\% < I_w < 9\%$ $0.7 < TKE < 1.0 \text{ m}^2 \text{ s}^{-2}$
convective	Lower wind speeds, low shear in swept-area, high amount of turbulence	low	low: $0.0 < \alpha < 0.1$	high: $13\% < I_U < 20\%$; $9\% < I_w < 17\%$ $1.0 < TKE < 1.4 \text{ m}^2 \text{ s}^{-2}$
strongly convective	Lowest wind speeds, very little wind shear in swept-area, highly turbulent	lowest	lowest: $\alpha < 0.0$	highest: $I_U > 20\%$; $I_w > 17\%$; $TKE > 1.4 \text{ m}^2 \text{ s}^{-2}$

Table 1: Thresholds for wind shear and turbulence during the five major stability classes, as well as associated boundary layer properties.

Figures

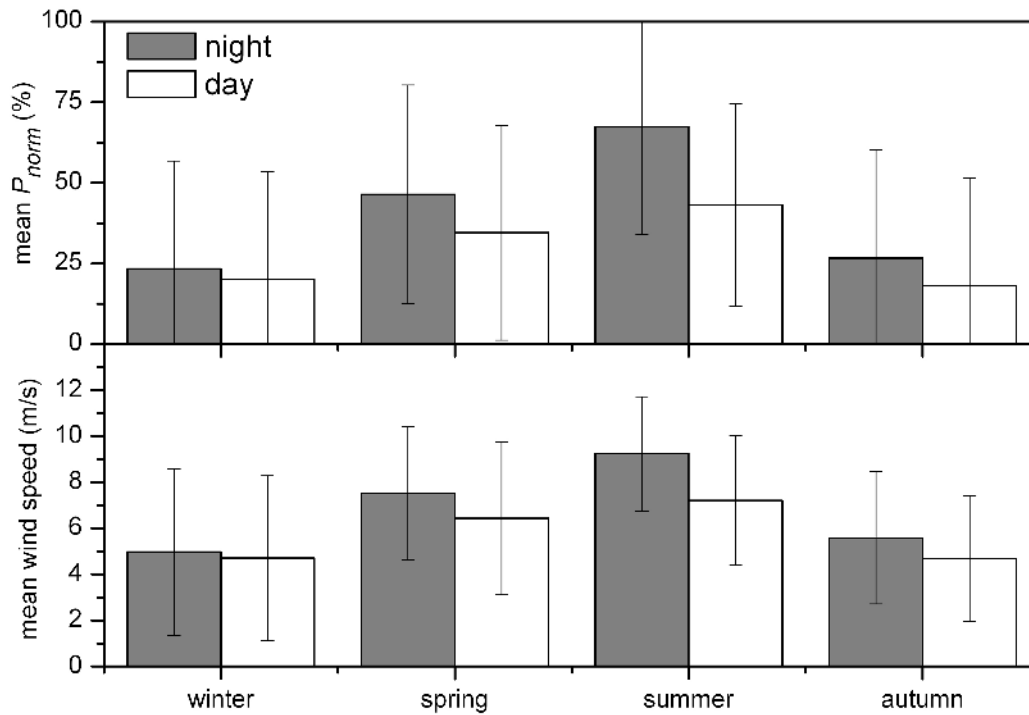


Figure 1: Mean seasonal (\pm one standard deviation) normalized power (P_{norm}) and nacelle (80 m) wind speed for all six turbines during nighttime and daytime hours. This site experiences strongest hub-height wind speeds and power production during summer nights while wind speed and power production are minimal during autumn and winter months.

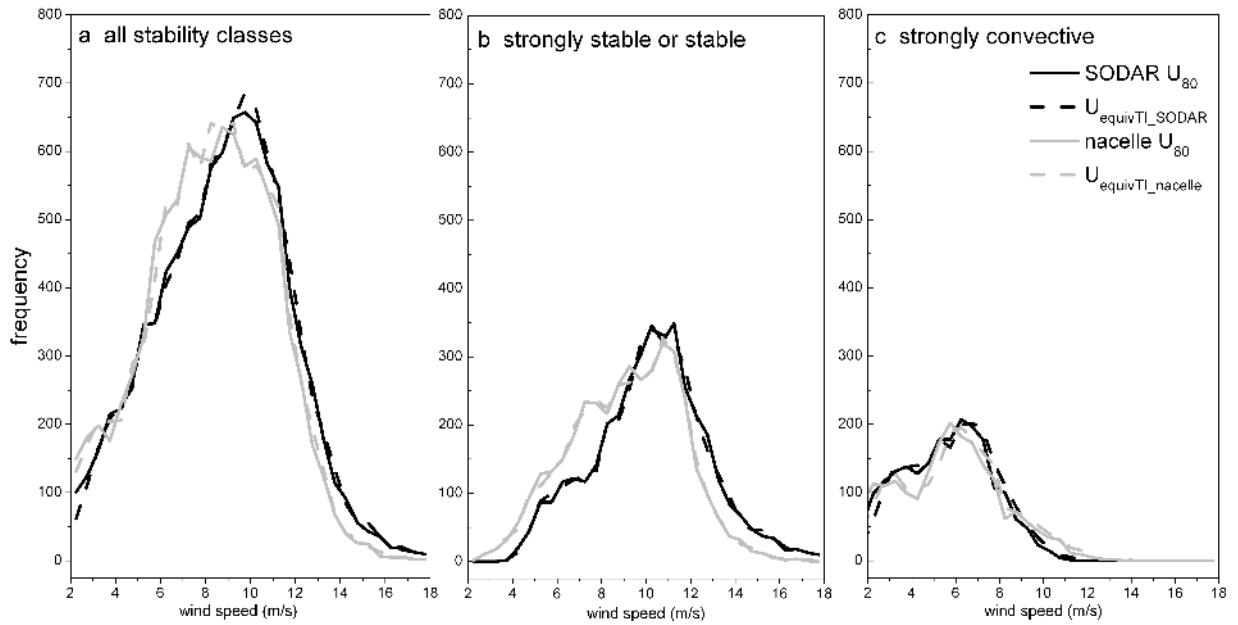


Figure 2: Frequency (# of events) of 10-minute SODAR 80 m, SODAR “true-flux” equivalent, nacelle hub-height, and nacelle-adjusted “true-flux” equivalent wind speed for Turbine 1 during the spring and summer months. Data are from (a) all stability periods, (b) periods of low turbulence, and (c) periods of high turbulence. The distributions of cup anemometer data are shifted to the left (towards lower wind speeds) during all times except under high turbulence conditions.

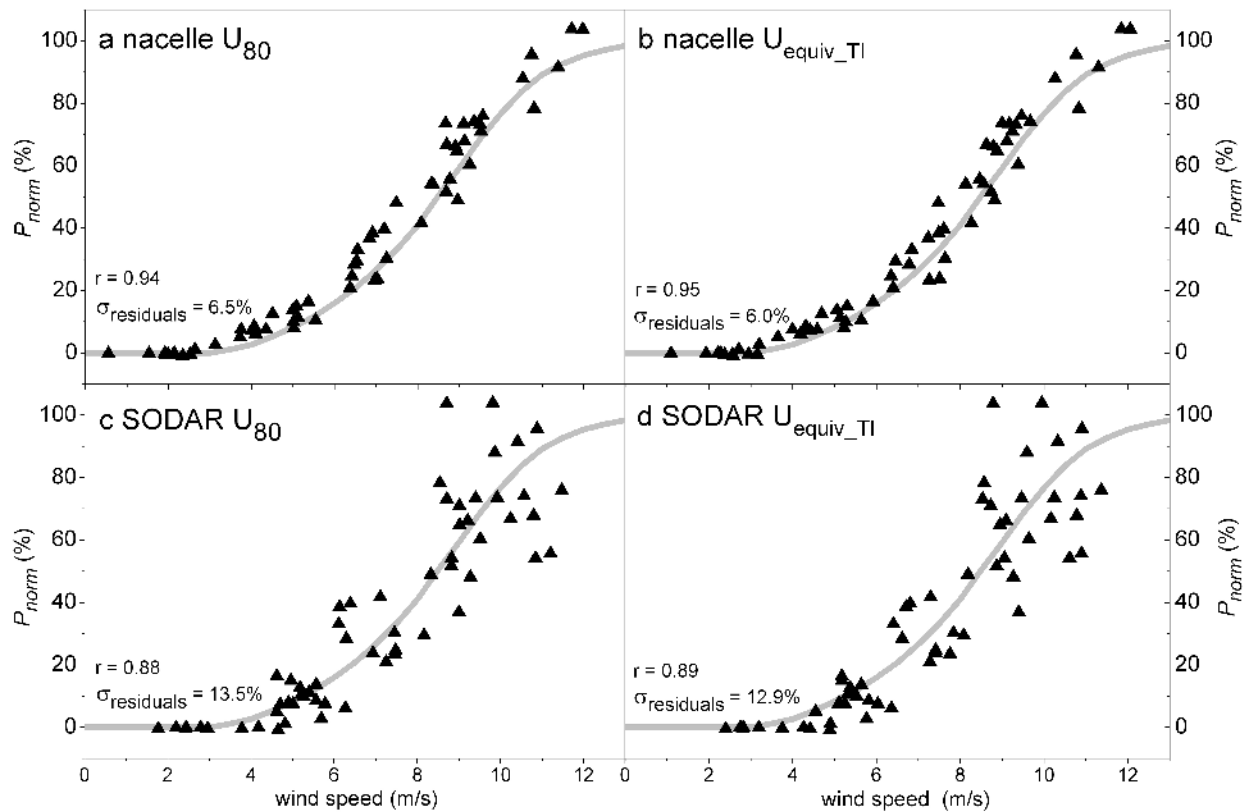


Figure 3: Power curves from a typical summer day based on 10-minute normalized power and (a) nacelle hub-height (80 m) wind speed, (b) nacelle-adjusted “true-flux” equivalent wind speed, (c) SODAR 80 m wind speed, and (d) SODAR “true-flux” equivalent wind speed. The nacelle and power data are from Turbine 1. Power curve accuracy is based on the “best fit” metrics (Pearson r value and standard deviation of residuals) between the observations and the manufacturer expected power curve. The plots show that $U_{equivTI_nacelle}$ produces the most accurate power curves at this site.

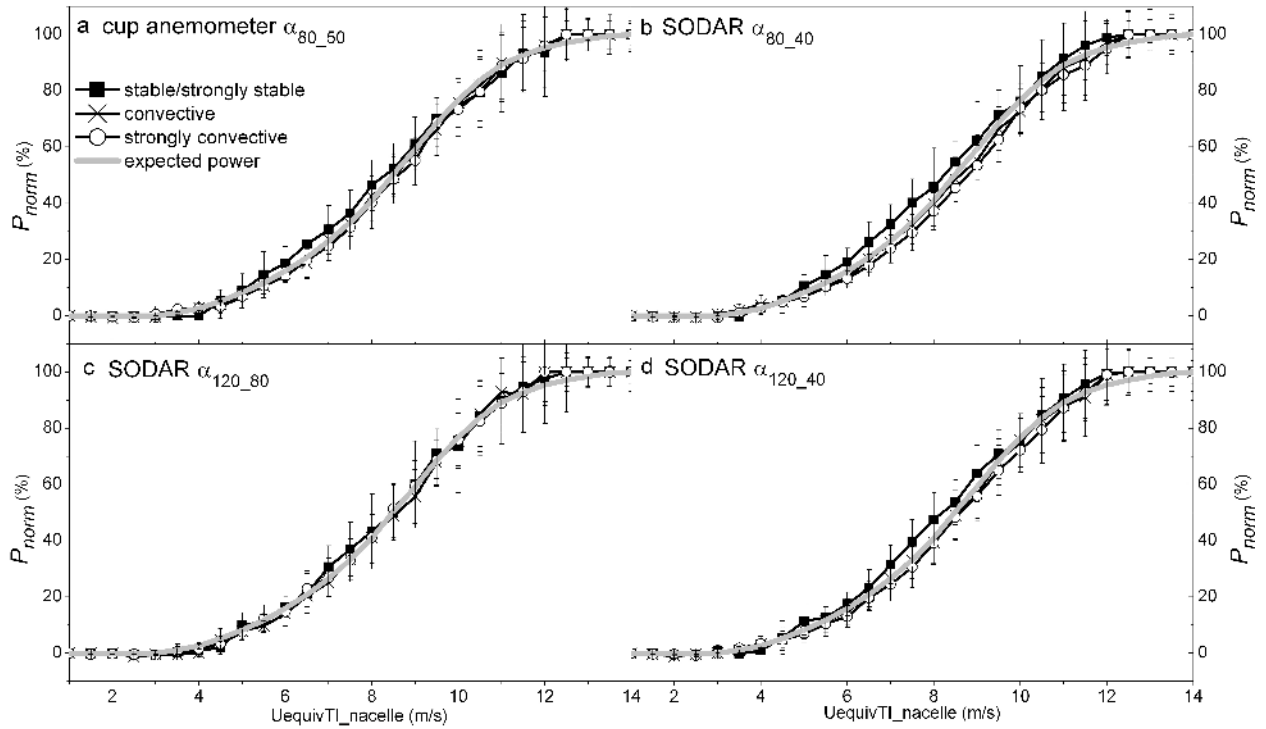


Figure 4: α -stratified power curves for Turbine 1 during strongly convective ($\alpha < 0.0$), convective ($0.0 < \alpha < 0.1$), and stable or strongly stable ($\alpha > 0.2$) atmospheric conditions. Wind shear is based on (a) meteorological tower and (b) SODAR measurements at heights in the lower half of the rotor disk, (c) SODAR measurements at heights in the upper half of the disk, and (d) SODAR measurements at heights across the entire disk. Plotted is mean normalized power \pm one standard deviation for each 0.5 m s^{-1} wind velocity bin as well as the manufacturer expected power curve.

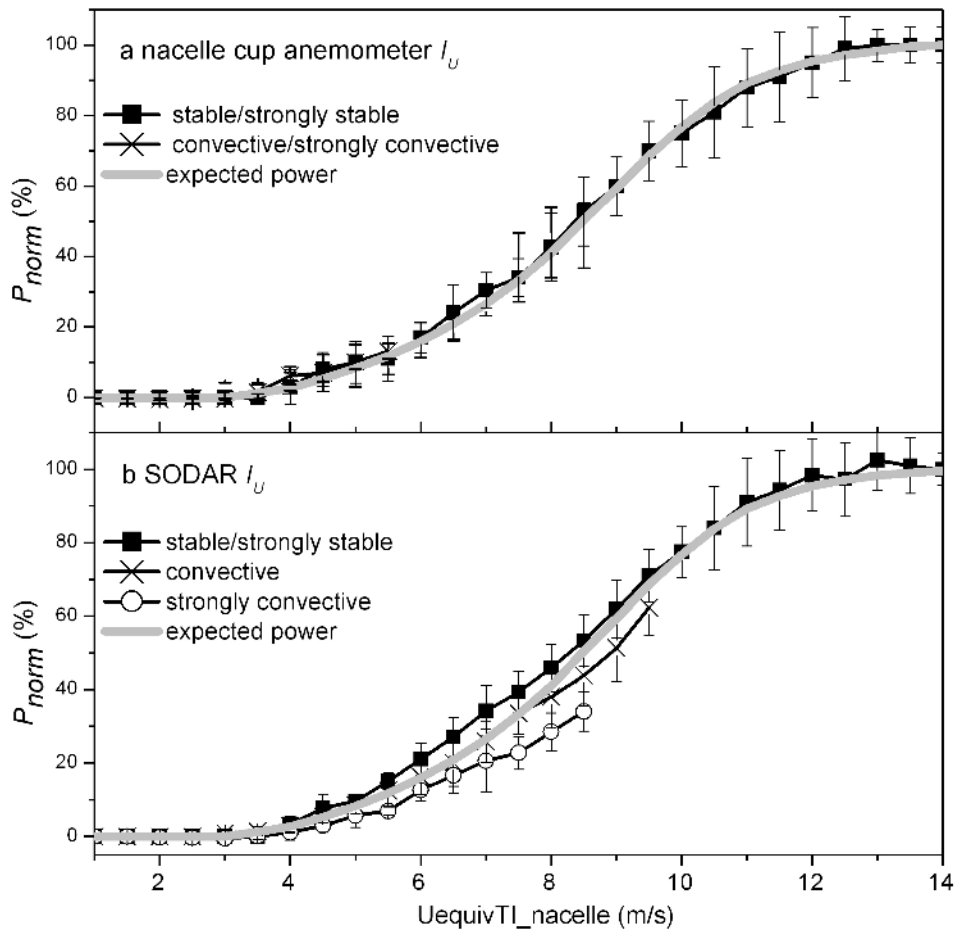


Figure 5: Stability-stratified power curves for Turbine 1 based on (a) nacelle 80 m cup anemometer I_U and (b) 80 m SODAR I_U during strongly stable or stable ($I_U < 10\%$), convective ($I_U > 13\%$, 8a) or ($13\% < I_U < 20\%$, 8b), and strongly convective ($I_U > 20\%$, 8b) conditions, as well as the manufacturer expected power curve. Too few data points were available to plot power observations during strongly convective conditions for the nacelle-based stability (8a).

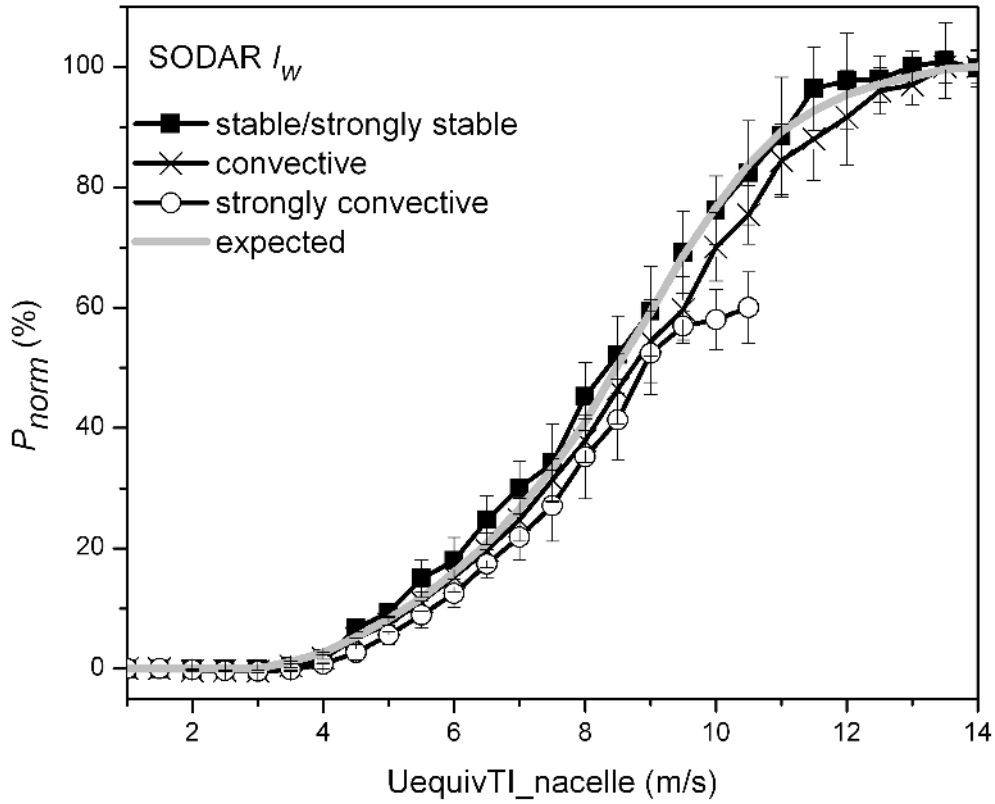


Figure 6: I_w -stratified power curves for Turbine 1 during strongly convective ($I_w > 17\%$), convective ($9\% < I_w < 17\%$), and stable or strongly stable ($I_w < 6\%$) conditions, as well as the expected power curve. Underperformance is observed during strongly convective conditions, especially for higher wind speeds.

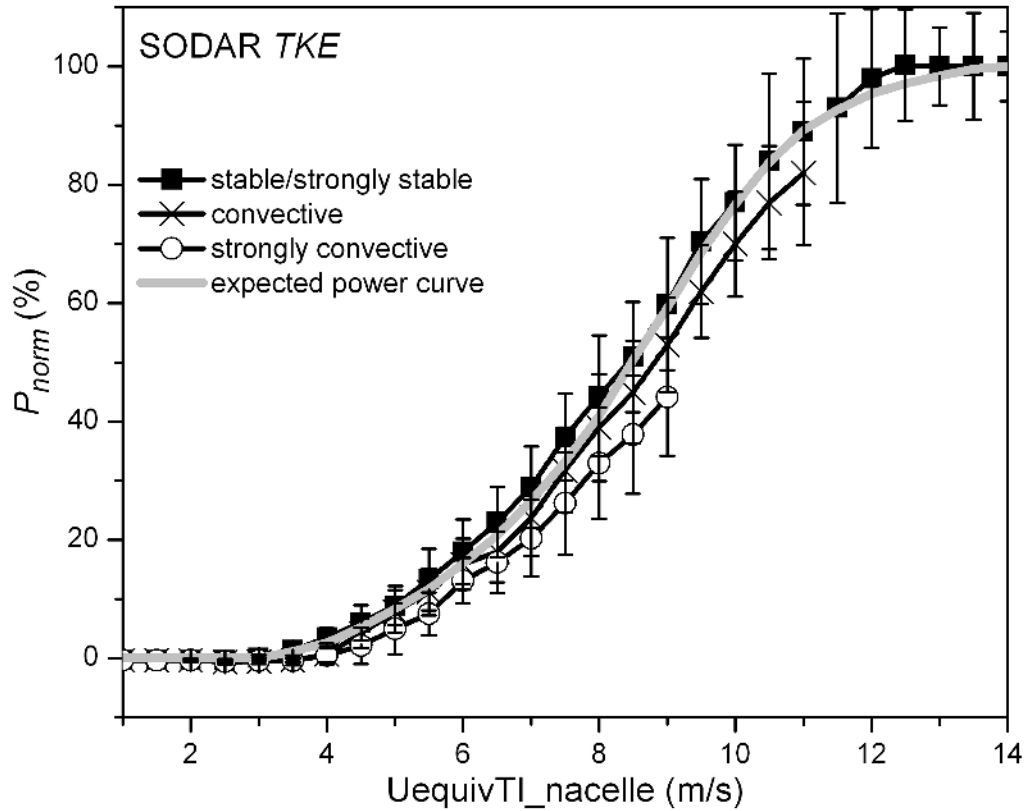


Figure 7: *TKE*-stratified power curves for Turbine 1 during strongly stable or stable ($TKE < 0.7 \text{ m}^2 \text{ s}^{-2}$), convective ($1.0 \text{ m}^2 \text{ s}^{-2} < TKE < 1.4 \text{ m}^2 \text{ s}^{-2}$), and strongly convective conditions ($TKE > 1.4 \text{ m}^2 \text{ s}^{-2}$). Also plotted is the manufacturer expected power curve. Stability-related underperformance is again observed at higher wind speeds for strongly convective conditions.